

# Finite Element Analysis of Contact Stress in a Full-metallic Pipe Joint for Hydrogen Pipelines

NAN BU, NAOHIRO UENO, and OSAMU FUKUDA  
 Measurement Solution Research Center  
 National Institute of Advanced Industrial Science and Technology (AIST)  
 807-1, Shuku-machi, Tosu, Saga, 841-0052  
 JAPAN  
 n.bu@aist.go.jp

*Abstract:* Hydrogen gas has been widely recognized as an environmentally clean and renewable energy fuel, and it provides a way to reduce greenhouse gas and air pollution emission. A great deal of effort has been made to develop new techniques in the field of hydrogen energy, including hydrogen production, storage, and infrastructure. Recently a metallic gasket, which is made of type 316L stainless steel, has been developed for hydrogen pipelines and pressure vessels. Contact stress analysis is important to verify structural strength of pipe joints using this gasket and to determine service parameters in order to achieve sufficient sealing performance.

This paper reports a preliminary study on contact stress analysis of a full-metallic bolted flange joint with the metallic gasket in bolt-up conditions. Because of shape and size of the contact interface in this pipe joint, direct measurement of the contact stress is difficult. Therefore, contact stress analyses have been performed numerically using a three-dimensional (3D) finite element method. The analytical object is a bolted flange joint for stainless steel pipes (Nominal size: 38 mm). 3D solid model was made up with CAD modeling software, Pro/Engineer. Then, analyses were performed in a commercial finite element analysis environment, ANSYS Workbench. The numerical results indicate a localized distribution of contact stress on the gasket's surface. In addition, a well-controlled bolt pretension is crucial for this gasket to prevent plastic deformation in the materials.

*Key-Words:* Metallic gasket, pipe joint, hydrogen pipelines, contact stress analyses, finite element model (FEM).

## 1 Introduction

With the exhaustion of traditional energy sources and the deterioration in global warming situation, there is an increasing demand for new environmentally clean energy fuel. Hydrogen gas has been widely recognized as a promising alternative energy source [1]. There have been a large number of researches carried out throughout the world in order to develop storage and transportation techniques for hydrogen energy [2]–[5].

Pipe joints are essential components in pipelines used for hydrogen gas infrastructure. Rubber materials have long predominated the field of static sealing technology, they are also frequently utilized in hydrogen pipelines. However, internal fracture (also called as blister fracture) may occur in rubber materials when high-pressure hydrogen gas is decompressed rapidly. O-rings, made of ethylene-propylene rubber (EPDM) and nitrile-butadiene rubber (NBR), have been tested in hydrogen gas environment (upto 10 MPa) [6], [7]. In addition, blister fracture of rubber materials has been reported in high-pressure environments of other gases [8], [9]. Considering the in-

creasing pressure levels of hydrogen gas used in fuel cell systems, much more development and investigation are required for rubber materials.

On the other hand, austenitic stainless steels (SS), especially those have good austenite stability (e.g., type 316L SS), are promising candidates for material of gaskets in hydrogen pipelines [10], [11]. A new type of metal gasket has been proposed, by Toki Engineering Co., Ltd., in order to replace traditional (rubber) O-rings [12]. Flanges or pipes used with this metal gasket have a circular groove on their end faces. The metal gasket's sealing surface contacts tangentially with the inner edge of flange's groove to perform sealing function (see Fig. 1). When the gasket and pipes are made of type 316L SS, we can apply this pipe joint to hydrogen pipelines.

Strength and tightness are the most important characteristics to a pipe joint. A large number of studies have been carried out to investigate stress distribution and sealing performance of pipe joints [13]–[16]. In the pipe joint studied in the present paper, since the gasket and pipes are made of same material (i.e., they have similar stiffness), all contacting parts are tough

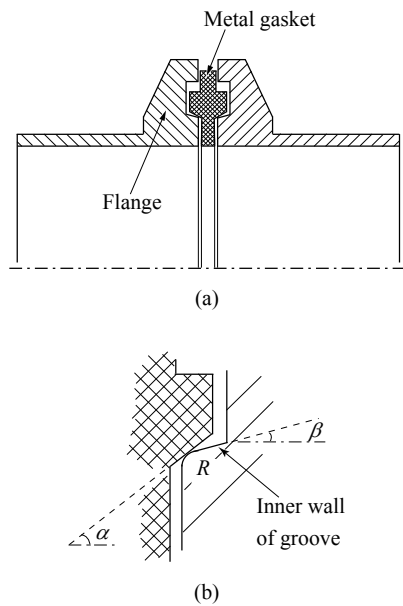


Figure 1: Schematic view of a pipe joint using the metal gasket. (a) Cross-section of a pipe joint assembled with two grooved flanges. (b) An enlarged view of the contact between the metal gasket and edge of the inner flange groove wall.

and deformable, plastic deformation caused by excessive contact stress would lead to leakage. For this reason, analyses of the contact stresses and strength of the pipe joint are extremely important to prevent it from leakage and seal failure. To the authors' knowledge, however, there is still no detailed investigation on contact stress analysis carried out for this gasket. The lack of thorough investigation has so far remarkably hindered business promotion of this product and reduced the potential for further improvement of the gasket's sealing properties.

In the present paper, contact stress analyses for a full-metallic bolted flange joint in bolt-up conditions are evaluated to reveal the distribution of contact stresses and the strength performance. Due to the narrow and small areas of contact in this pipe joint, direct measurement of stress is very difficult. Therefore, three-dimensional finite element analyses (FEA) have been carried out in an ANSYS Workbench environment to estimate the stress and deformation developed in the contact zone during bolt-up process.

The rest of this paper is organized as follows: Section 2 briefly introduces the metal gasket and characteristics of the full-metallic bolted flange joint. The finite element model and configurations used in the simulation are explained in Section 3. Section 4 shows the numerical results of FEA. Finally, Section 5 concludes this paper.

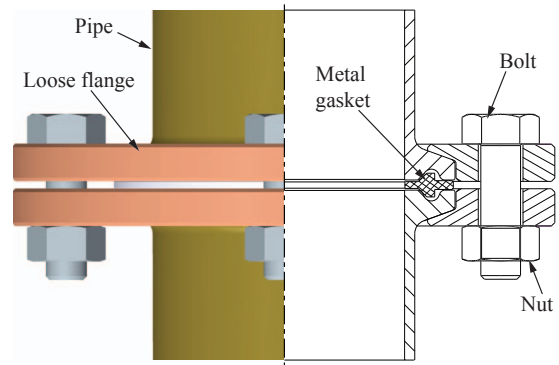


Figure 2: A bolted flange joint using the metal gasket.

## 2 A Full-metallic Pipe Joint

### 2.1 The Metal Gasket

The metal gasket is ring-shaped. It has two conical faces on both contact sides, the cone has a half angle of  $\alpha$ . This gasket is designed for mating with flanges, which have a circular groove on their end faces. Fig. 1 depicts a schematic view of a pipe joint that consists of the metal gasket and two grooved flanges. It should be noted that the edge of groove wall is usually smoothed with a rounded corner, which has a small radius  $R$ . For example,  $R$  is specified as 0.8 mm in the standard ISO 2852 [17].

In Fig. 1.(b), the inner groove edge of pipe has a convex cross-sectional profile, while the gasket's contact surface has a linear cross-sectional profile. Specifying the angle of the inner wall of flange groove with respect to the radial axis of the flange as  $\beta$ , the rounded edge contacts tangentially with the gasket's conical face if  $\alpha > \beta$ .

When the gasket's axis matches with the axes of pipes, a circular contact line is generated under a just-touching condition. If clamping force is applied to the pipe joint, deformation occurs in the contact areas of the abutting parts, as a result, sealing zones are formed between the conical faces and the groove edges in the flanges on both sides.

### 2.2 Geometry of a Bolted Flanged Joint

For pipe joints like the one shown in Fig. 1.(a), clamping can be achieved with an adjustable two or three-part clamp or two loose flanges. This paper studies a pipe joint clamped with two loose flanges using four bolts. Geometry of this bolted flange joint is illustrated in Fig. 2. The right part gives a cross-sectional view.

Contact stress analyses in this study were performed with a bolted flange joint for stainless steel pipes (Nominal size: 38 mm) [17]. Some major di-

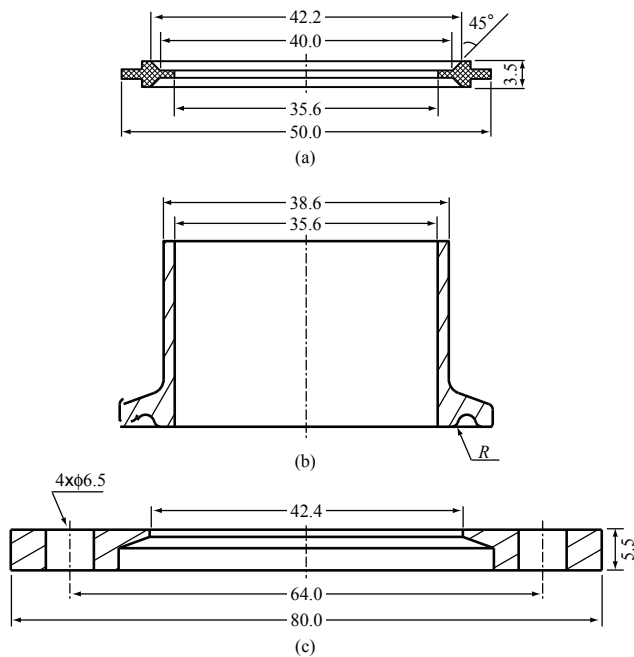


Figure 3: Major dimensions of parts in the pipe joint. (a) Metal gasket, (b) Pipe with grooved end face, (c) Loose flange.

mensions of the parts are given in Fig. 3. Four M6 size bolts were used to clamp up this flange joint. In this gasketed pipe joint,  $\alpha = 45^\circ$  and  $\beta = 23^\circ$ . End face of the pipe fitting follows the standard ISO 2852, for detailed dimensions of the end face and the groove, please refer to Ref. [17].

A three-dimensional (3D) solid model was made up for the pipe joint using Pro/Engineer (Wildfire 3.0). In this model, each bolt-nut pair was treated as a single entity. The geometric model was then imported into an ANSYS Workbench (Release 11.0 SP1) to achieve finite element analyses.

### 3 Finite Element Modeling of a Full-metallic Bolted Flange Joint

#### 3.1 Finite Element Model

Although the pipe joint has cyclically symmetrical geometric characteristics with respect to the common radial axis of the components, since ANSYS Workbench does not support simulation of cyclically symmetric model, which is a basic sector model of a full geometry (e.g., a quarter model for the pipe joint in this paper), the analyses were performed with a full 3D finite element (FE) model. The solid model was meshed with SOLID186, SOLID187, CONTA174, and TARGE170 element types. A  $180^\circ$  segment of the FE model is depicted in Fig. 4. After a bolt-

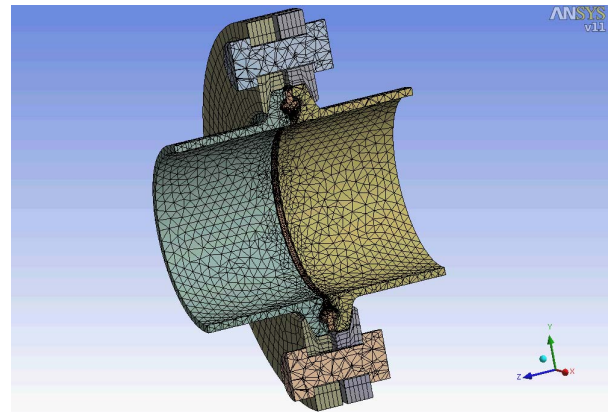


Figure 4: A  $180^\circ$  segment of the meshed finite element model for a bolted flange joint with the metal gasket.

up process, the contact area would be a narrow circular ring. In order to evaluate this localized contact stress distribution between the metal gasket and the pipes, meshing was emphasized on these contact surfaces. Size control was applied to these contact surfaces with an element size of 0.1 mm. The total number of elements in the FE models is in the range of 1,233,591 - 1,676,278, and node number is about 732,792 - 1,006,710. Fig. 5 shows a detailed mesh of the contact surfaces on the gasket and the pipe end faces ( $R = 0.8$  mm).

For simulation of the contact stress between the gasket and pipes, frictionless contact type was used as contact condition. Even though the geometry was created in just-touching condition, due to meshing and numerical round-off in the models, both initial gaps and penetration were formed in the contact areas before bolt pretension was applied. The option of interface treatment was set as "adjust to touch". In addition, pure penalty method was utilized for the contact formulation method in order to reduce the computation time and to facilitate convergence in the simulations.

On the other hand, bonded contact type was chosen as contact condition for the contact surfaces between pipes and loose flanges and the contact pairs between bolt-nut sets and loose flanges.

#### 3.2 Material Properties

Stainless steel type 316L was used as the material for all parts in the stress analyses of the bolted flange joint. The Young's modulus  $E$  is 190 GPa, the Poisson's ratio  $\nu$  is 0.29, and the yield strength  $\sigma_y$  is 206.81 MPa [18].

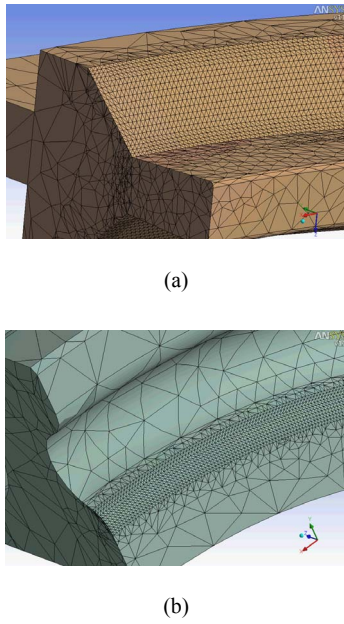


Figure 5: A detailed mesh of a finite element model. (a) The metal gasket, (b) Pipe end face.

### 3.3 Loading and Boundary Conditions

In this study, only the bolt-clamping load was added to the joint. During assembly process, deformation and displacement of the pipes and the loose flanges are symmetric with respect to the gasket. The pipes and flanges are free to move in both the axial and the radial directions. Cylindrical supports were applied to the outer cylindrical faces of the pipes and the flanges (radial and axial directions: free; tangential direction: fixed). At the meanwhile, the gasket was constrained in the axial and tangential directions.

Pretension of bolts can be easily applied in the ANSYS Workbench environment. The force applied to each bolt is defined as  $F_B$ . The pretension load was set as 250, 400, and 500 N in the following FE analyses.

## 4 Simulation Results

### 4.1 Distribution of Contact Stress

For description of the contact stress distribution, a cylindrical coordinate system  $(r, \theta, z)$  is defined; the cylindrical axis is set aligning with the common axis of the pipe joint and origin of the cylindrical coordinate system is on the middle plane of the metal gasket. The metal gasket contacts with the pipes at the initial contact line,  $r_c = 20.312$  mm, before bolt pretension is applied. Figure 6 depicts the distribution of Z-axis normal stress on one contact surface of the metal gasket with  $F_B = 400$  N. Variations of the Z-axis normal

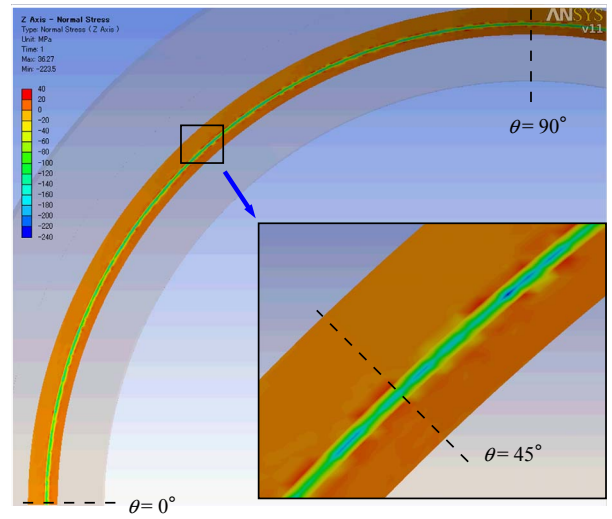


Figure 6: Distribution of Z-axis normal stress on a quarter  $[0^\circ, 90^\circ]$  of one contact surface of the metal gasket ( $F_B = 400$  N).

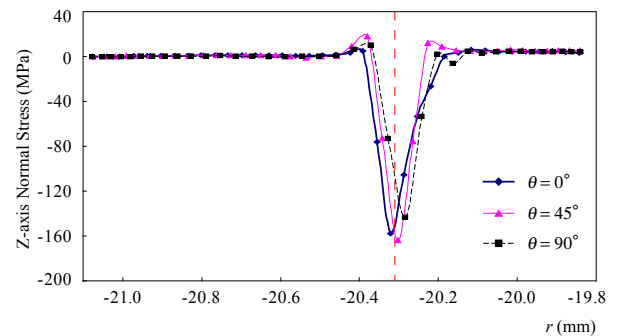


Figure 7: Z-axis normal stresses for  $\theta = 0^\circ, 45^\circ$  and  $90^\circ$  in Fig. 6. A red dashed line makes the radial distance  $r_c$ .

stress along the radial direction are shown in Fig. 7, for nodes on the angular position  $\theta = 0^\circ, 45^\circ$ , and  $90^\circ$ , respectively. A narrow zone of negative contact stresses can be found on the contact surface, width of the contact zone in the radial direction is about two element size (0.2 mm). In addition, for each  $\theta$  the Z-axis normal stress reaches its negative peak at positions close to the initial contact line.

### 4.2 Strength of the Bolted Flange Joint

Proper strength is required to ensure suitable functions of a bolted flange joint in all service conditions. After the bolt-up process, both stress and deformation on the interface between the gasket and the pipe reach their maximum values. When internal pressure is further applied to this pipe joint, load in the bolts increases while stress in the contact zone decreases. If plastic

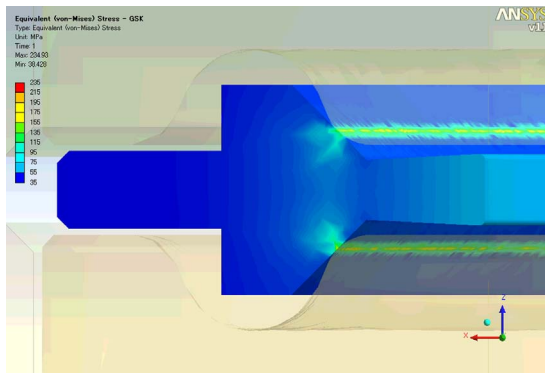


Figure 8: Equivalent stress in the gasket for  $F_B = 500$  N.

deformation occurs due to the bolt pretension, locations in the contact zone, which have plastic deformation, may be easy to result in leakage and seal failure.

Equivalent stress is used to predict yielding in the material. The equivalent stress  $\sigma_e$  is defined as follows,

$$\sigma_e = \sqrt{\frac{(\sigma_1 - \sigma_2)^2 + (\sigma_2 - \sigma_3)^2 + (\sigma_3 - \sigma_1)^2}{2}} \quad (1)$$

In this bolted flange joint, maximum equivalent stress is found in the gasket. Contour plot of equivalent stresses in the gasket, under the pretension load in each bolt  $F_B = 500$  N, is shown in Fig. 8. The nodes in the contact zone on the gasket's contact surface have relatively large equivalent stresses. The maximum equivalent stress is 234.93 MPa  $>$   $\sigma_y$ . In this case, there are locations in the contact zone that undergo permanent deformation caused by excessive contact stresses.

For  $F_B = 400$  and 250 N, the maximum equivalent stress is 190.27 and 123.44 MPa, respectively. Deformation of the gasket is in the elastic range, so that full recovery is possible for these cases. It should be noted that full recovery of the metal gasket enable it to be *reusable*, this is a promising characteristic especially for pipeline in industrial applications.

## 5 Conclusion

The aim of this study is to evaluate stress condition of a novel metal gasket in a full-metallic bolted flange joint developed for hydrogen pipelines. Stress analyses were carried out using a 3D finite element method (FEM). As the first step of this research, FE analyses reported in this paper were carried out using a simulation software package, ANSYS DesignSpace. Although the results obtained may not be absolutely accurate, the numerical analyses offer engineering data

to help us in understanding properties of the metal gasket. The numerical results of FE analyses confirm that the contact stress occurs in a concentrated contact zone, spreading over a narrow ring on the conical surface of the gasket. In addition, A relatively small clamping force, e.g.,  $F_B = 500$  N, can lead to plastic deformation in the material of type 316L stainless steel. These results provide valuable information to orientate further improvement on the present design.

In the future research, we would like to improve the simulation accuracy, and we plan to achieve non-linear FE analysis for the metal gasket. Also, FE analysis with a simplified model is an interesting solution. Furthermore, real experimental test is needed to verify performance of the metal gasket.

**Acknowledgements:** This work is partly supported by Fukuoka Industry Science and Technology (Fukuoka IST) Foundation on *The Development of Full-metallic Pipe Connections for Hydrogen Pipelines*. The authors would like to thank Toki Engineering Co., Ltd. for the collaboration.

## References:

- [1] G. Nicoletti, The hydrogen option for energy: A review of technical, environmental and economic aspects, *Int. J. Hydrogen Energ.* 20, 1995, pp. 759–765.
- [2] B. Sakintuna, F. Lamari-Darkrim, and M. Hirscher, Metal hydride materials for solid hydrogen storage: A review, *Int. J. Hydrogen Energ.* 32, 2007, pp. 1121–1140.
- [3] C. Yang and J. Ogden, Determining the lowest-cost hydrogen delivery mode, *Int. J. Hydrogen Energ.* 32, 2007, pp. 268–286.
- [4] M. Pentimalli, F. Padella, A. La Barbera, L. Piloni, and E. Imperi, A metal hydride-polymer composite for hydrogen storage applications, *Energ. Convers. Manag.* 50, 2009, pp. 3140–3146.
- [5] Y. Peet, P. Sagaut, and Y. Charron, Pressure loss reduction in hydrogen pipelines by surface restructuring, *Int. J. Hydrogen Energ.* 34, 2009, pp. 8964–8973.
- [6] J. Yamabe, M. Nakao, and H. Fujiwara, S. Nishimura, Influence of fillers on hydrogen penetration properties and blister fracture of EPDM composites exposed to 10 MPa hydrogen gas, *Trans. Jpn Soc. Mech. Eng. A* 74, 2008, pp. 971–981. (in Japanese)
- [7] J. Yamabe and S. Nishimura, Influence of fillers on hydrogen penetration properties and blister

- fracture of rubber composites for O-ring exposed to high-pressure hydrogen gas, *Int. J. Hydrogen Energ.* 34, 2009, pp. 1977–1989.
- [8] A. Stevenson and G. Morgan, Fracture of elastomers by gas decompression, *Rubber Chem. Tech.* 68, 1995, pp. 197–211.
- [9] P. Embury, High-pressure gas testing of elastomer seals and a practical approach to designing for explosive decompression service, *Sealing Technology* 2004(6), 2004, pp. 6–11.
- [10] G. Han, J. He, S. Fukuyama, and K. Yokogawa, Effect of strain-induced martensite on hydrogen environment embrittlement of sensitized austenitic stainless steels at low temperatures, *Acta Mater.* 46, 1998, pp. 4559–4570.
- [11] K. Kawamoto, K. Ochi, Y. Oda, and H. Noguchi, Effects of hydrogen gas environment on the fatigue strength at  $10^7$  cycles in the plain specimens of type 316L stainless steel (A report focusing on the behavior of micro fatigue crack), *Trans. Jpn. Soc. Mech. Eng. A* 73, 2007, pp. 1343–1350. (in Japanese)
- [12] M. Tomiki, *Pipe Joints*, Japan Patent 4157493, 2008.
- [13] H. Estrada and I.D. Parsons, Strength and leakage finite element analysis of a GFRP flange joint, *Int. J. Pres. Ves. Pip.* 76, 1999, pp. 543–550.
- [14] T. Fukuoka and T. Takaki, Three-dimensional finite element analysis of pipe flange connections: Effects of solid-metal flat gasket, *Trans. Jpn Soc. Mech. Eng. A* 66, 2000, pp. 651–657. (in Japanese)
- [15] S. Kurokouchi, S. Morita, and M. Okabe, Characteristics of a taper-seal type gasket for the Conflat sealing system, *J. Vac. Sci. Technol. A* 19, 2001, pp. 799–802.
- [16] E. Roos, H. Kockelmann, and R. Hahn, Gasket characteristics for the design of bolted flange connections of metal-to-metal contact type, *Int. J. Pres. Ves. Pip.* 79, 2002, pp. 45–52.
- [17] ISO 2852, Stainless steel clamp pipe couplings for the food industry, 2nd edition, 1993.
- [18] IDAC Ltd., IDAC ANSYS Workbench material database V1.01, 2006.